Published in final edited form as:
Acta Oncol. 2008 ; 47(5): 906–916. doi:10.1080/02841860701843050.

Is it beneficial to selectively boost high-risk tumor subvolumes? A comparison of selectively boosting high-risk tumor subvolumes versus homogeneous dose escalation of the entire tumor based on equivalent EUD plans

Yusung Kim[1] and **Wolfgang A. Tomé**[2]

[1]Department of Radiation Oncology, University of Iowa, Iowa City, U.S.A

[2]Departments of Human Oncology and Medical Physics, University of Wisconsin, Madison, U.S.A

Abstract

Purpose—To quantify and compare expected local tumor control and expected normal tissue toxicities between selective boosting IMRT and homogeneous dose escalation IMRT for the case of prostate cancer.

Methods—Four different selective boosting scenarios and three different high-risk tumor subvolume geometries were designed to compare selective boosting and homogeneous dose escalation IMRT plans delivering the same equivalent uniform dose (EUD) to the entire PTV. For each scenario, differences in tumor control probability between both boosting strategies were calculated for the high-risk tumor subvolume and remaining lower-risk PTV, and were visualized using voxel based iso-TCP maps. Differences in expected rectal and bladder complications were quantified using radiobiological indices (generalized EUD (gEUD) and normal tissue complication probability (NTCP)) as well as %-volumes.

Results—For all investigated scenarios and high-risk tumor subvolume geometries, selective boosting IMRT improves expected TCP compared to homogeneous dose escalation IMRT, especially when lack of control of the high-risk tumor subvolume could be the cause for tumor recurrence. Employing, selective boosting IMRT significant increases in expected TCP can be achieved for the high-risk tumor subvolumes. The 3 conventional selective boosting IMRT strategies, employing physical dose objectives, did not show significant improvement in rectal and bladder sparing as compared to their counterpart homogeneous dose escalation plans. However, risk-adaptive optimization, utilizing radiobiological objective functions, resulted in reduction in NTCP for the rectum when compared to its corresponding homogeneous dose escalation plan.

Conclusions—Selective boosting is a more effective method than homogeneous dose escalation for achieving optimal treatment outcomes. Furthermore, risk-adaptive optimization increases the therapeutic ratio as compared to conventional selective boosting IMRT.

Keywords

Functional imaging; selective boosting; dose painting; TCP; IMRT

Address of Correspondence: Dr. Wolfgang A. Tomé, University of Wisconsin, School of Medicine and Public Health, Departments of Human Oncology and Medical Physics, K4/314 CSC, 600 Highland Ave., Madison, WI 53792, U.S.A., Tel: 001-608-263-8510, Fax: 001-608-263-9947, tome@humonc.wisc.edu.

INTRODUCTION

Recent prospective, randomized trials have demonstrated that radiotherapy (RT) doses of less or equal to 70 Gy delivered in 2Gy fractions are inadequate for curative treatment of clinically localized prostate cancers [1,2,3,4]. Moreover, RT doses in excess of 76 Gy delivered in 2Gy fractions are associated with extended survival rates and reduced incidence of distant metastases as well as improvements in both biochemical and clinical local control of prostate cancer [5,6]. As a result, many dose escalation trials for prostate cancer have been designed and carried out [cf. 7–12]. Zelefsky and colleagues reported administering 86.4 Gy to the planning target volume (PTV) using intensity-modulated radiotherapy (IMRT) and observed at 24-month follow-up the same toxicity rate for 86.4 Gy IMRT and 81 Gy IMRT—indicating that for IMRT tumor dose can be escalated above prescription dose levels that have been found tolerable for 3D conformal radiotherapy [7]. A uniform target dose has been pursued in dose escalation trials since the physiologic makeup of the target has been assumed to be reasonably similar throughout. In reality, however a considerable spatial variation in radiobiological characteristics exists throughout the treatment target—e.g. extent of tumor hypoxia, tumor cell proliferation, and tumor cell density. Thus, one may label homogenous dose escalation a form of ‘anatomic’ boosting IMRT in view that its nescient nature ignores the existence of intratumoral high-risk subvolumes.

An alternative way of dose escalation recently proposed is selective boosting or dose painting. Selective boosting utilizes functional or molecular imaging modalities to effectively deliver radiation doses to achieve optimum RT outcome [13]. Tomé and Fowler found using modeling that significant increases up from 50% to 75% in tumor control probability (TCP) can be achieved for a small increase in the risk of necrosis, if tumor subvolumes comprising 60–80% of the entire tumor are selectively boosted by 20 to 30% above the minimal peripheral dose surrounding the entire tumor volume [14]. Pioneering studies in planning [8,15] and clinical practice [9–12,16] using functional imaging have followed.

However, a comparison of selective boosting IMRT and homogeneous dose escalation IMRT, has not been carried out for plans delivering the same equivalent uniform dose (EUD) to the entire treatment target. Thus, the purpose of this study was to quantify which treatment strategy is more effective in achieving optimal RT outcome in terms of local tumor control and normal tissue sparing. We have generated a selective boosting and a homogeneous dose escalation IMRT plan for four different boosting scenarios and for three different high-risk tumor subvolume geometries. The resulting treatment plans were compared using both physical-dose-volume measures and bio-effect measures to determine the possible improvement in the therapeutic ratio for these techniques for different target geometries.

METHODS AND MATERIALS

IMRT Treatment Planning

The Philips Pinnacle^3 treatment planning system (TPS) (Philips Medical Systems, Fitchburg, Wisconsin), version 8.1u, was employed in the generation of all treatment plans. The same equiangular beam arrangement consisting of seven coplanar fields, dose grid of 0.4 cm × 0.4 cm × 0.4 cm, and fraction size (2 Gy per fraction) were used for all investigated planning strategies (cf. Table 1). A 0.5 cm volumetric margin was added to the clinical target volume (CTV) to obtain the PTV and a similar margin was employed for the high-risk tumor subvolume (nodule) when contracting from PTV to rPTV (a remaining low risk PTV without nodule).

To carry out a comprehensive comparison of selective boosting and homogeneous dose escalation for prostate cancer, we have constructed four different boosting scenarios (i.e. scenario 1–4 in Table 1)]. For each selective boosting IMRT plan, a corresponding

homogeneous dose escalation IMRT plan was generated, having the same EUD for the entire PTV. Table 1 summarizes boosting levels and prescribed doses to the entire PTV for each scenario. Scenario 1 and 2 are based on recent clinical studies [9–12]. Scenario 3 was designed to study a more aggressive selective boosting IMRT strategy employing physical dose objectives. While scenario 4 represents risk-adaptive optimization, which has been recently proposed by us [8], we have chosen our parameters such that the minimal peripheral dose surrounding the entire PTV is larger or equal to the standard IMRT dose prescription for prostate cancer [6].

Three different high-risk tumor subvolume geometries were also constructed for each boosting scenario. Figure 2 shows the high-risk tumor subvolumes, here after referred to as nodules, which have been constructed in the posterior peripheral zone of the prostate. [9] The location of the nodules has been based on the literature—since it has been reported that 74% of prostate cancer foci are located in the area ventral to the rectum [17].

OAR constraints for scenario 1 and 2 were chosen such that the resulting DVHs satisfied all clinical criteria set forth for the selective boosting strategies reported in [9–12]. Organs-at-risk (OAR) constraints for scenario 3 were obtained from the Memorial Sloan Kettering Cancer Center dose-escalation experience for prostate cancer and correspond to the 86.4 Gy prescription dose level to the entire PTV [7]. Each homogeneous dose escalation plan employed the same (OAR) constraints as its corresponding selective boosting plan.

Risk-Adaptive Optimization

With selective boosting IMRT, boosting levels for high risk tumor subvolumes are chosen in one of three ways: 1) based on clinical experience (i.e. a clinician determined a boosting level in terms of a physical dose), which represents the majority of present approaches [10–12,16], 2) based on functional imaging intensity for high-risk tumor subvolumes (i.e. the prescription function is deduced from functional imaging intensities) [13,15], and 3) based on radiobiological optimal trade-off between TCP and NTCP by using clinical parameters [8, 18].

Risk-adaptive optimization is an example of the third method of selective boosting while the other three selective boosting strategies (scenario 1, scenario 2, and scenario 3) studied in this paper are examples of the first method. In risk-adaptive optimization, attention is given to the risk levels of different tumor subvolumes which are identified using a form of functional imaging. The risk of a tumor subvolume is assessed by specifying clinical parameters for tumor control such as the dose at which 50% of tumors are controlled (D_{50}) and the relative slope of the dose response curve (γ_{50}). Since a detailed discussion of risk-adaptive optimization has been presented in Ref. 8, only portions relevant to the current discussion are repeated here.

Risk-adaptive optimization uses the clinical parameters (D_{50} and γ_{50}) as its optimization parameters instead of physical dose-volume constraints. Thus, the following tumor subvolume risk classifications were used in this study (cf. Table 2): intermediate (M: $D_{50} = 72.8Gy$), high (H: $D_{50} = 77.3Gy$), and very high (H_+: $D_{50} = 82.3Gy$). These D_{50} values are motivated by the recently published data of Levegrün *et al.* [19]. Levegrün and colleagues fit the prostate biopsy outcome to TCP models for favorable, intermediate, and unfavorable prostate tumors for 102 patients, and estimated D_{50} for each prognostic tumor case. They used three prognostic factors (T-stage, Gleason score, and prostate specific antigen (PSA) level) to classify the risk of a prostate tumor. For nodules that are assumed to exhibit risk attributes such as rapid proliferation, rapid metabolism, or hypoxia, a very high (H_+: $D_{50} = 82.3Gy$) was assumed for the one and the large nodule geometries, while a high (H: $D_{50} = 77.3Gy$) and very high risk (H_+: $D_{50} = 82.3Gy$) was assumed for the two-nodule geometry. The rPTV was assumed to exhibit an intermediate risk classification (M: $D_{50} = 72.8Gy$). A steep dose-response curve

value ($\gamma_{50} = 8$) was employed for nodule and rPTV. For OAR constraints, we have chosen the recent clinical data and values listed in Table 2 [20,21].

Subvolume-based TCP Evaluation and Voxel based Iso-TCP maps

To quantify the expected local tumor control for prostate cancer, we have calculated TCP values for the nodule, rPTV, and the entire PTV. We have chosen a subvolume-based TCP model (Eq. 5 in Ref. 8), utilizing a Poisson TCP model reparameterized in terms of D_{50} and γ_{50} (cf. Table 1 in Ref. 22). As a novel RT plan evaluation tool, a voxel iso-TCP map has been developed to visualize tumor control probability distributions and iso-tumor-control lines.

Voxel-based NTCP Evaluation

To calculate NTCP values, the Lyman-NTCP model employing generalized equivalent uniform dose (gEUD) was used as a DVH reduction method (i.e. reducing non-uniform dose maps characterized by their DVH to equivalent uniform dose maps) as suggested by Rancati *et al.* [20]:

$$\mathrm{NTCP(gEUD)}=\frac{1}{\sqrt{2\pi}}\int_{-\infty}^{t}\exp\left(-\frac{u^2}{2}\right)\mathrm{du},\ t=\frac{(\mathrm{gEUD}-D_{50})}{\mathrm{mD}_{50}},\ \text{and}\ \ \mathrm{gEUD}=\left(\sum_i v_i D_i^{\frac{1}{n}}\right)^n \tag{1}$$

where D_{50} is the dose to the whole organ that leads to a complication probability of 50%. In Eq. (1) v_i denotes the fractional volume of the i^{th} dose bin whose dose value is denoted by D_i, m denotes the parameter relating to the slope of NTCP curve, and n denotes the volume effect parameter. This gEUD based Lyman-NTCP model is mathematically equivalent to the classical Lyman-Kutcher-Burman model [24] (cf. Appendix A. of Ref. 20). Table 2 shows the NTCP model parameters. To minimize the dependency on NTCP model parameters, the rectum NTCP values have been evaluated using three different sets of NTCP model parameters that have been recently published by Rancati *et al.* [20] and Tucker *et al.* [25].

RESULTS

Comparisons of Local Tumor Control between selective boosting and homogeneous dose escalation IMRT

As shown in Figure 1 and 2, independent of boosting scenario and tumor subvolume geometry, the selective boosting IMRT plans seem to be more beneficial than their corresponding homogeneous dose escalation IMRT plans in terms of increased local tumor control probability for the high-risk tumor subvolumes. The advantage of selective boosting IMRT was especially maximized in the predicted local tumor control of the high-risk tumor subvolume.

Expected TCP values High-risk tumor subvolumes

For scenario 1, independent of high-risk tumor subvolume geometry, selective boosting IMRT did yield an expected TCP above 90% for the high-risk tumor subvolume, as compared to an expected TCP of 1.8% maximally for homogeneous dose escalation IMRT in which the same EUD is delivered to the entire PTV as with selective boosting IMRT (cf. Figure 1 and 2). For scenario 2, scenario 3, and scenario 4 (risk-adaptive optimization), we found when using selective boosting IMRT the expected TCP for the different high risk tumor subvolume geometries could be increased from 26 – 41%, 26 – 36%, and 25 – 30%, respectively, over those that could be achieved with homogeneous dose escalation IMRT delivering the same EUD to the entire PTV as selective boosting.

As clearly visualized in the voxel based iso-TCP maps (cf. Figure 2), independent of nodule geometry the expected TCP that could be achieved in the tumor subvolumes having the highest risk classification when employing homogeneous dose escalation was less than 74% (also cf. Figure 1 in this respect). In particular, the homogeneous dose escalation plans corresponding to selective boosting scenario 3 showed TCP values of less than 67%, while those corresponding to scenarios 1 and 2, showed severely unfavorable TCP values of less than 1.8% for high-risk tumor subvolumes.

Expected TCP values for the rPTV and entire PTV

As one can see from the middle panel of Figure 1 independent of nodule geometry only scenarios 3 and 4 appear to deliver an adequate minimal peripheral dose the entire PTV to yield an expected TCP above 90% for the chosen intermediate risk classification of the rPTV for either selective boosting or homogeneous dose escalation IMRT. While in scenarios 1 and 2 for the chosen intermediate risk classification of the rPTV and independent of nodule geometry, the minimal peripheral dose delivered to the entire PTV is to low to yield clinically acceptable expected TCP values for the rPTV for either selective boosting or homogenous dose escalation IMRT (cf. middle panel of Figure 1). Since the minimal peripheral dose delivered to the entire PTV is to low it appears that homogenous dose escalation is advantageous in this case since it yields higher expected TCP values in the rPTV than selective boosting (cf. middle panel of Figure 1), this advantage, however disappears once the expected TCP values for the entire PTV are considered (cf. bottom panel of Figure 1). Showing that independent of nodule geometry selective boosting yields higher overall expected TCP values even in the face of insufficient minimal peripheral dose to the entire PTV to yield clinically acceptable expected TCP values.

If however, a sufficiently high minimal peripheral dose is delivered to the entire PTV to yield TCP values in excess of 90% for the rPTV as is the case for scenarios 3 and 4, then independent of nodule geometry homogeneous dose escalation plans show favorable tumor control values of over 90%, and therefore the benefit of selective boosting IMRT appears to be diminished (cf. Figure 1 bottom panel). However, it should be borne in mind that tumors are the ultimate parallel structures, and are controlled if, and only if, all tumor subvolumes are controlled [26]. Therefore, as illustrated in Figure 2, instead of the entire PTV one should consider the highest risk tumor subvolume, having the most unfavorable TCP value when trying to minimize the risk of possible tumor recurrence. As can be clearly seen from the voxel iso-TCP maps presented in Figure 2, only selective boosting scenario 4 (risk-adaptive optimization), utilizing radiobiological objective functions provides a more uniform expected local tumor control probability across the entire PTV for all high-risk tumor subvolume geometries investigated than either conventional selective boosting IMRT or homogeneous dose escalation IMRT.

Comparisons of Normal Tissue Sparing between Selective boosting and Homogeneous Dose Escalation

As shown in Table 3 and Figure 3, risk-adaptive optimization showed a noticeable improvement in rectal and bladder sparing when compared to its counterpart homogeneous dose escalation plan—a decrease in expected NTCP for the rectum by up to 5.3%, and a decrease in the rectal volume (rectal wall volume) irradiated to intermediate doses (40 – 60 Gy) of up to 16.4% (10.7%) across the different nodule geometries as shown in Table 3 and Figure 3. While risk-adaptive optimization plans showed expected NTCP values of less than 5.4% for the both rectal volume and rectal wall volume for all three NTCP parameter sets, their corresponding homogeneous dose escalation plans appeared to have the highest expected NTCP values of up to 9.2%. With regard to bladder complications, risk-adaptive optimization again showed better sparing, as indicated by a decrease in bladder volume irradiated above of 75 Gy by up to 4.7%, while selective boosting scenario 3 that is most closely matched in its expected tumor effect showed a decrease by up to 0.7%.

For the other three selective boosting strategies, the OAR sparing of the rectum and bladder did not show noticeable differences between selective boosting and homogeneous dose escalation IMRT (cf. Figure 3).

With regard to late rectal bleeding, all %-volume data (irradiated to least the specified dose) for selective boosting and homogeneous dose escalation were within the suggested criteria in the literature. The values of V_{70Gy} (the %-volume that received at least 70 Gy) for selective boosting IMRT and homogeneous dose escalation IMRT were found to be less than 19.5% and 22.0% of the rectal volume, respectively—satisfying the criteria of $V_{70Gy} < 26.2\%$ [27]. Jackson *et al.* [28] and Fiorino *et al.* [29] suggested that the risk of late rectal bleeding could also be associated with large volumes irradiated to intermediate doses (40 – 60 Gy), suggesting the following cutoff values for the rectal wall: $V_{40Gy} < 60\%$, $V_{50Gy} < 60\%$, and $V_{60Gy} < 50$ ~55%. The values of V_{40Gy}, V_{50Gy}, and V_{60Gy} for the rectal wall were less than 34.8%, 19.6%, and 13.8% for selective boosting plans and less than 37.6%, 21.2%, and 14.3% for homogeneous dose escalation plans, respectively, for all high-risk tumor subvolume geometries investigated. With regard to late genitourinary complications, bladder toxicity values from all investigated selective boosting and homogeneous dose escalation strategies were within the criteria of $V_{65\sim75Gy} < 20\%$ as reported in the literature [30]. The highest values of V_{65Gy} and V_{75Gy} for all four scenarios were 13.8% and 9.2%.

DISCUSSION

Our study shows that selective boosting IMRT can considerably improve expected local tumor control as compared to homogeneous dose escalation IMRT (cf. Figure 1 and 2). Even though selective boosting delivers the same EUD to the entire PTV as is done in the corresponding homogeneous dose escalation it is more effective in terms of expected local tumor control as evidenced by voxel based iso-TCP maps, since it more effectively distributes dose across the different tumor subvolumes. In other words, part of the dose seems to be wasted in the case of homogeneous dose escalation IMRT, which is shown clearly in the voxel based iso-TCP maps (cf. Figure 2) and may not be so readily apparent from isodose distributions or dose volume histograms. Our results are consistent with published data where selective boosting and homogeneous dose escalation strategies are compared [31,32,33]. Thorwarth and colleagues recently showed that a dose-painting (selective boosting IMRT) strategy resulted for head-and-neck (H&N) cancer in the most favorable TCP estimate of 70.2% as compared to 57.7% and 55.9% obtained using an additional uniform-boosting strategy, in which the fluorodeoxyglucose (FDG)-PET positive volume is boosted (homogeneous dose escalation) [31]. Using a physical dose measure (mean dose) to build equivalent plans between selective boosting IMRT and homogeneous dose escalation IMRT, Malinen and coworkers [32] and Yang and Xing [33] have carried out comparison studies for H&N cancer and prostate cancer. Malinen and coworkers [32] suggested a selective boosting IMRT strategy that focuses on hypoxic tumor subvolumes for head-and-neck cancer, which gave a three times higher expected TCP than that which could be obtained using homogeneous dose escalation IMRT. For specific tumor subvolumes in prostate cancer, Yang and Xing [33] obtained expected TCP values of less than 0.6% and 40.8 ~ 58.7% for mean doses of 70 Gy and 81 Gy employing homogeneous dose escalation IMRT while selective boosting IMRT yielded TCP values in excess of 99%.

With regard to normal tissue complications, only risk-adaptive optimization, utilizing radiobiological objective functions (TCP, NTCP, and UTCP) showed significant improvements in rectal and bladder sparing when compared to its EUD equivalent homogeneous dose escalation plan. On the other hand, the other three selective boosting strategies, employing conventional physical (dose-volume) objective functions did not show any improvement in terms of OAR sparing to their corresponding homogeneous dose escalation plans. This result is consistent with the papers by Mohan and coworkers [34,35], which suggest

that pure physical objective functions are not sufficient, and therefore radiobiological objective functions should be incorporated to achieve optimum treatment outcome.

We have chosen to work with equivalent EUD rather than equivalent physical dose (same mean dose) to generate homogeneous dose escalation plans that are equivalent to their corresponding selective boosting plans in terms of the EUD delivered to the entire PTV, since for constant mean dose but increasing dose inhomogeneity in the target one obtains decreasing EUD estimates (cf. Figure 2 in Niemierko [36]). Therefore, physical mean dose without specifying the allowed degree of dose inhomogeneity may not be a good metric for plan comparison, since it could yield widely differing TCP estimates depending on the degree of dose inhomogeneity achieved in the dose painting treatment plan. However, treatment plans having the same EUD are part of an equivalence class of plans having an equivalent number of surviving clonogens, which should at least in theory result in equivalent tumor control [36].

Selective boosting IMRT assumes the use of some form of functional imaging. Thus, selective boosting IMRT inherently incorporates the advantages associated with functional imaging—i.e. possible delineation of high-risk tumor subvolumes and target volume (GTV)—and thus may lead to a reduced target volume and increased sparing of OARs. Furthermore, selective boosting IMRT holds the promise of delivering boost dose only to those patients in need of the additional dose for tumor control. Independent of the selective boosting method selected, in selective boosting IMRT regions to be boosted are patient-specific. In contrast to selective boosting IMRT, homogeneous dose escalation IMRT delivers boost doses in a non-patient-specific manner. The underlying assumption of homogeneous dose escalation is that a higher dose correlates with a higher tumor control. This invokes the therapeutic problem that if all patients were treated with a homogeneous dose escalation technique, a large number of them would incur added side effects from the additional dose even though they were already destined for local control without boosting. Moreover, if a functional imaging technique is available that allows one to subdivide the tumor volume into a class of tumor subvolumes of different risk classifications then voxel based iso-TCP maps appear to be a more adequate tool for treatment plan evaluation than physical isodose distributions, since they more directly related to expected local tumor control.

CONCLUSIONS

Our study shows that functional image-guided, selective boosting IMRT considerably improves local tumor control when compared to anatomic image-guided, homogeneous dose escalation IMRT. Employing selective boosting IMRT, it is possible to achieve significant increases in TCP for high-risk tumor subvolumes as compared to homogeneous dose escalation IMRT delivering the same EUD to the entire PTV as selective boosting IMRT. Only risk-adaptive optimization plans, using biological objective functions, appeared to have better OAR sparing than their corresponding homogeneous dose escalation plans, showing a reduction in expected NTCP for the rectum while the other three selective boosting strategies, employing conventional physical (dose-volume) objective functions did not show an improvement in OAR sparing. Selective boosting allows one to deliver dose more effectively to achieve optimal radiotherapy treatment outcome as evidenced by improved voxel iso-TCP maps, which could lead to increased local control for localized advanced cancer. Moreover, risk-adaptive optimization, using biological objective functions promises an increased therapeutic ratio in contrast to other selective boosting IMRT strategies, employing conventional IMRT optimization using physical dose-volume objective functions.

Acknowledgments

This work was partially supported by the research grant for Philips Radiation Oncology Systems and the National Institute of Health R01-CA109656.

REFERENCES

1. Zietman AL, DeSilvio M, Slater JD, et al. A randomized trial comparing conventional dose (70.2GyE) and high-dose (79.2 GyE) conformal radiation in early stage adenocarcinoma of the prostate: Results of an interim analysis of RTOG 95-09. Proc Am Soc Ther Radiol Oncol 2004;60:S131–S132.
2. Pollack A, Zagars GK, Smith LG, et al. Preliminary results of a randomized radiotherapy dose-escalation study comparing 70 Gy with 78 Gy for prostate cancer. J Clin Oncol 2000;18:3904–3911. [PubMed: 11099319]
3. Sathya JR, Davis IR, Julian JA, et al. Randomized trial comparing iridum implant plus external-beam radiation therapy with external-beam radiation therapy alone in node-negative locally advanced cancer of the prostate. J Clin Oncol 2005;23:1192–1199. [PubMed: 15718316]
4. Lukka H, Hayter C, Julian JA, Warde P, et al. Randomized trial comparing two fractionation schedules for patients with localized prostate cancer. J Clin Oncol 2005;23:6132–6138. [PubMed: 16135479]
5. Jacob R, Hanlon AL, Horwitz EM, Movsas B, Uzzo RG, Pollack A. The relationship of increasing radiotherapy dose to reduced distant metastases and mortality in men with prostate cancer. Cancer 2004;100:538–543. [PubMed: 14745870]
6. Pollack A, Zagars GK, Starkschall G, et al. Prostate cancer radiation dose response: Results of the M.D. Anderson phase III randomized trial. Int J Radiat Oncol Biol Phys 2002;53:1097–1105. [PubMed: 12128107]
7. Zelefsky MJ, Fuks Z, Leibel SA. Intensity-modulated radiation therapy for prostate cancer. Semin Radiat Oncol 2002;12:229–237. [PubMed: 12118388]
8. Kim Y, Tomé WA. Risk-adaptive optimization: Selective boosting of high-risk tumor subvolumes. Int J Radiat Oncol Biol Phys 2006;66:1528–1542. [PubMed: 17126211]
9. De Meerleer G, Villeirs G, Bral S, et al. The magnetic resonance detected intraprostatic lesion in prostate cancer: planning and delivery of intensity-modulated radiotherapy. Radiother Oncol 2005;75:325–333. [PubMed: 15967524]
10. van Lin EN, Fütterer JJ, Heijmink SW, et al. IMRT boost dose planning on dominant intraprostatic lesions: gold marker-based three-dimensional fusion of CT with dynamic contrast-enhanced and ^{1}H-spectroscopic MRI. Int J Radiat Oncol Biol Phys 2006;65:291–303. [PubMed: 16618584]
11. Pickett B, Vigneault E, Kurhanewicz J, Verhey L, Roach M. Static field intensity modulation to treat a dominant intraprostatic lesion to 90 Gy compared to seven field 3-dimentional radiotherapy. Int J Radiat Oncol Biol Phys 1999;44:921–929. [PubMed: 10386651]
12. Xia P, Pickett B, Vigneault E, Verhey LJ, Roach M III. Forward or inversely planned segmental multileaf collimator IMRT and sequential tomotherapy to treat multiple dominant intraprostatic lesions of prostate cancer to 90 Gy. Int J Radiat Oncol Biol Phys 2001;51:244–254. [PubMed: 11516874]
13. Bentzen SM. Theragnostic imaging for radiation oncology: dose-painting by numbers. Lancet Oncol 2005;6:112–117. [PubMed: 15683820]
14. Tomé WA, Fowler JF. Selective boosting of tumor subvolumes. Int J Radiat Oncol Biol Phys 2000;48:593–599. [PubMed: 10974480]
15. Vanderstraeten B, Duthoy W, De Gersem W, De Neve W, Thierens H. [^{18}F] fluorodeoxy-glucose positron emission tomography ([^{18}F]FDG-PET) voxel intensity-based intensity-modulated radiation therapy (IMRT) for head and neck cancer. Radiother Oncol 2006;79:249–258. [PubMed: 16564588]
16. Chao KSC, Bosch WR, Mutic S, Lewis JS, et al. A novel approach to overcome hypoxic tumour resistance: Cu-ATSM-guided intensity-modulated radiation therapy. Int J Radiat Oncol Biol Phys 2001;49:1171–1182. [PubMed: 11240261]
17. Brenner DJ, Hall EJ. Fractionation and protraction for radiotherapy of prostate carcinoma. Int J Radiat Oncol Biol Phys 1999;43:1095–1101. [PubMed: 10192361]

18. Brahme A. Optimized radiation therapy based on radiobiological objectives. Semin Radiat Oncol 1999;9:35–47. [PubMed: 10196397]
19. Levegrün S, Jackson A, Zelefsky MJ, et al. Risk group dependence of dose-response for biopsy outcome after three-dimensional conformal radiation therapy of prostate cancer. Radiother Oncol 2002;63:11–26. [PubMed: 12065099]
20. Rancati T, Fiorino C, Gagliardi G, et al. Fitting late rectal bleeding data using different NTCP models: results from an Italian multi-centric study (AIROPROS0101). Radiother Oncol 2004;73:21–32. [PubMed: 15465142]
21. Burman C, Kutcher GJ, Emami B, Goitein M. Fitting of normal tissue tolerance data to an analytic function. Int J Radiat Oncol Biol Phys 1991;21:123–135. [PubMed: 2032883]
22. Bentzen SM, Tucker SL. Quantifying the position and steepness of radiation dose-response curves. Int J Radiat Biol 1997;71:531–542. [PubMed: 9191898]
23. Suit, HD.; Shalek, RJ.; Wette, R. Cellular Radiation Biology. Baltimore: Williams & Wilkins; 1965. Radiation response of C3H mouse mammary carcinoma evaluated in terms of cellular radiation sensitivity; p. 514-530.
24. Kutcher GJ, Burman C. Calculation of complication probability factors for non-uniform normal tissue irradiation: the effective volume method. Int J Radiat Oncol Biol Phys 1989;16:1623–1630. [PubMed: 2722599]
25. Tucker SL, Dong L, Cheung R, Johnson J, et al. Comparison of rectal dose-wall histogram versus dose-volume histogram for modeling the incidence of late rectal bleeding after radiotherapy. Int J Radiat Oncol Biol Phys 2004;60:1589–1601. [PubMed: 15590191]
26. Munro TR, Gilbert CW. The relation between tumour lethal doses and the radiosensitivity of tumour cells. Br J Radiol 1961;34:246–251. [PubMed: 13726846]
27. Huang EH, Pollack A, Levy L, et al. Late rectal toxicity: Dose-volume effects of conformal radiotherapy for prostate cancer. Int J Radiat Oncol Biol Phys 2002;54:1314–1321. [PubMed: 12459352]
28. Jackson A, Skwarchuk MW, Zelefsky MJ, et al. al. Late rectal bleeding after conformal radiotherapy of prostate cancer (II): Volume effects and dose-volume histograms. Int J Radiat Oncol Biol Phys 2001;49:685–698. [PubMed: 11172950]
29. Fiorino C, Cozzarini C, Vavassori V, et al. Relationships between DVHs and late rectal bleeding after radiotherapy for prostate cancer: Analysis of a large group of patients pooled from three institutions. Radiother Oncol 2002;64:1–12. [PubMed: 12208568]
30. Marks LB, Carroll PR, Dugan TC, Anscher MS. The response of the urinary bladder, urethra, and ureter to radiation and chemotherapy. Int J Radiat Oncol Biol Phys 1995;31:1257–1280. [PubMed: 7713787]
31. Thorwarth D, Eschmann S, Paulsen F, Alber M. Hypoxia dose painting by numbers: A planning study. Int J Radiat Oncol Biol Phys 2007;68:291–300. [PubMed: 17448882]
32. Malinen E, Søvik Å, Hristov D, Bruland ØS, Olsen DR. Adapting radiotherapy to hypoxic tumours. Phys Med Biol 2006;51:4903–4921. [PubMed: 16985278]
33. Yang Y, Xing L. Towards biologically conformal radiation therapy (BCRT): Selective IMRT dose escalation under the guidance of spatial biology distribution. Med Phys 2005;32:1473–1484. [PubMed: 16013703]
34. Wang X, Mohan R, Jackson A, Leibel SA, Fuks Z, Ling CC. Optimization of intensity-modulated 3D conformal treatment plans based on biological indices. Radiother Oncol 1995;37:140–152. [PubMed: 8747939]
35. Mohan R, Wang X, Jackson A, Bortfeld T, Boyer AL, et al. The potential and limitations of the inverse radiotherapy technique. Radiother Oncol 1994;32:232–248. [PubMed: 7816942]
36. Niemierko A. Reporting and analyzing dose distributions: A concept of equivalent uniform dose. Med Phys 1997;24:103–110. [PubMed: 9029544]

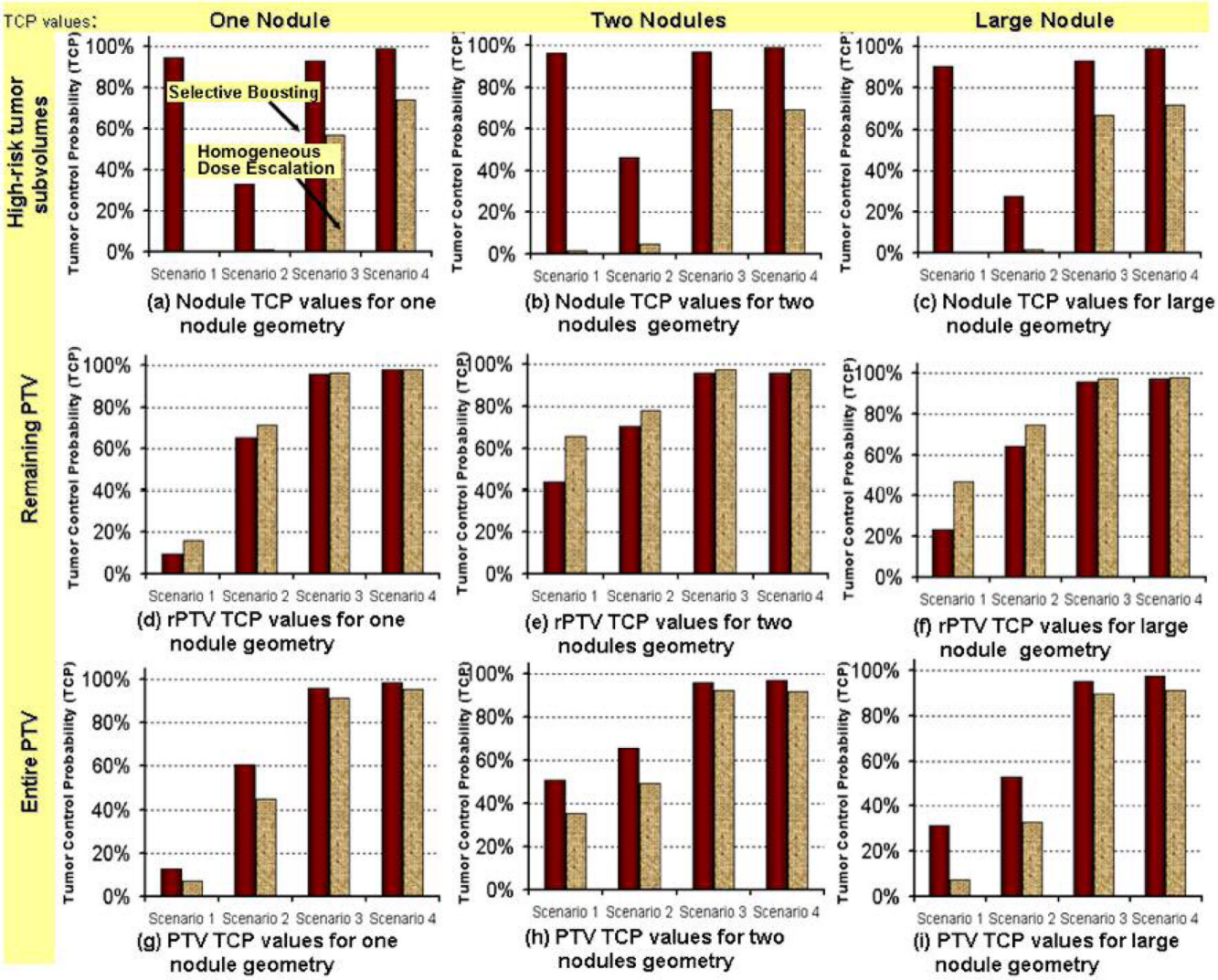

Figure1.

The three panels in the first row show the comparison of the expected the TCP values for the high-risk tumor subvolumes comparing selective boosting IMRT and homogeneous dose escalation IMRT for each scenario for each of the three different high-risk tumor subvolume geometries indicated. The expected TCP values for rPTV and PTV are similarly compared in the second and third row, respectively.

Abbreviations: Scenarios 1– 4 = stand for four different boosting strategies described in Table 1.

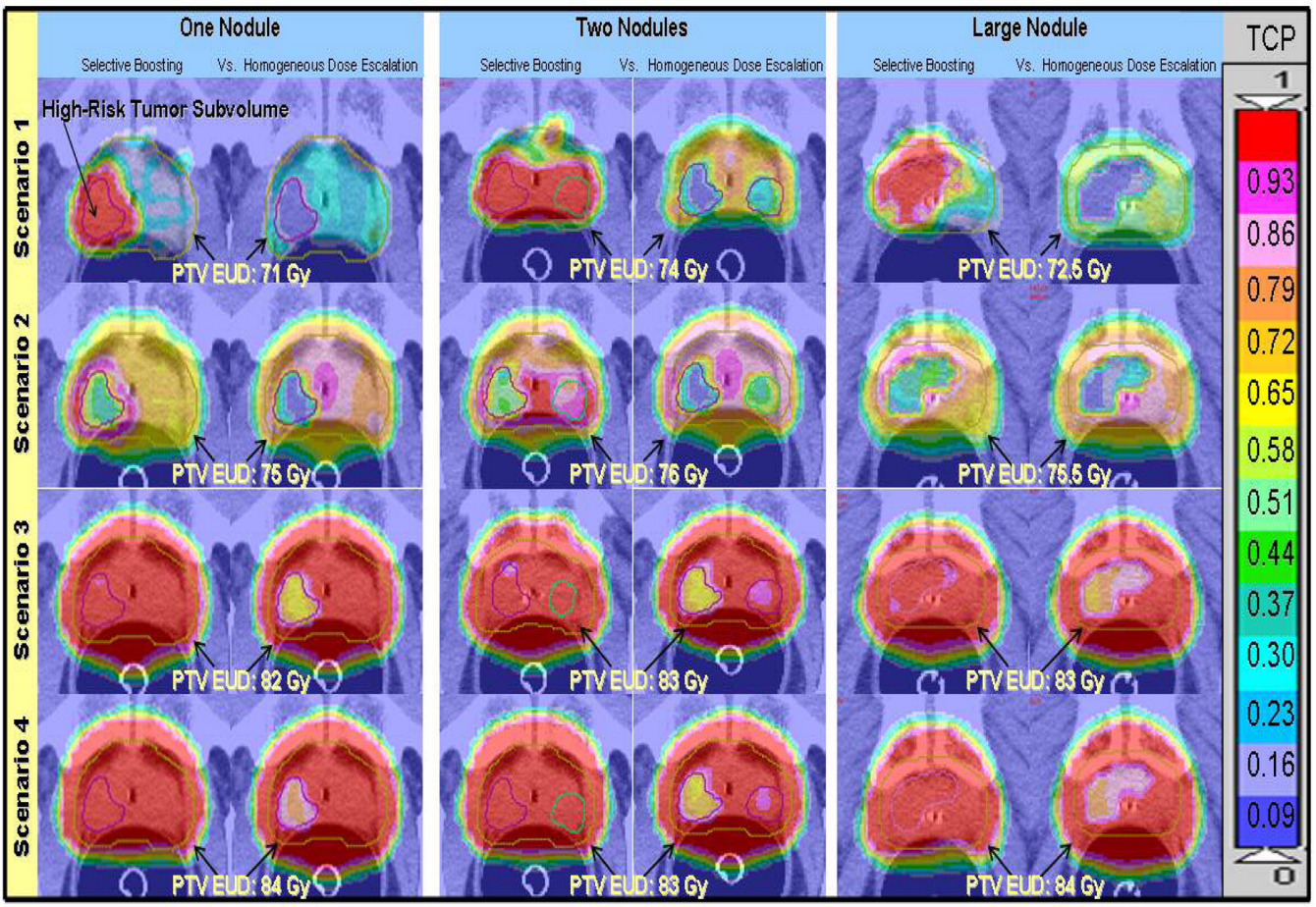

Figure2.

Voxel based iso-TCP maps of selective boosting IMRT and homogeneous dose escalation IMRT for the four different scenarios and the three different high-risk tumor subvolume geometries studied, where each voxel represent the local tumor control in terms of expected TCP. The benefit of selective boosting IMRT in terms of increased expected local tumor control is clearly visualized independent of high-risk tumor subvolume geometry. TCP values range from 0 to 1 and the upper bound of the TCP range for a given color are indicated on the color bar.

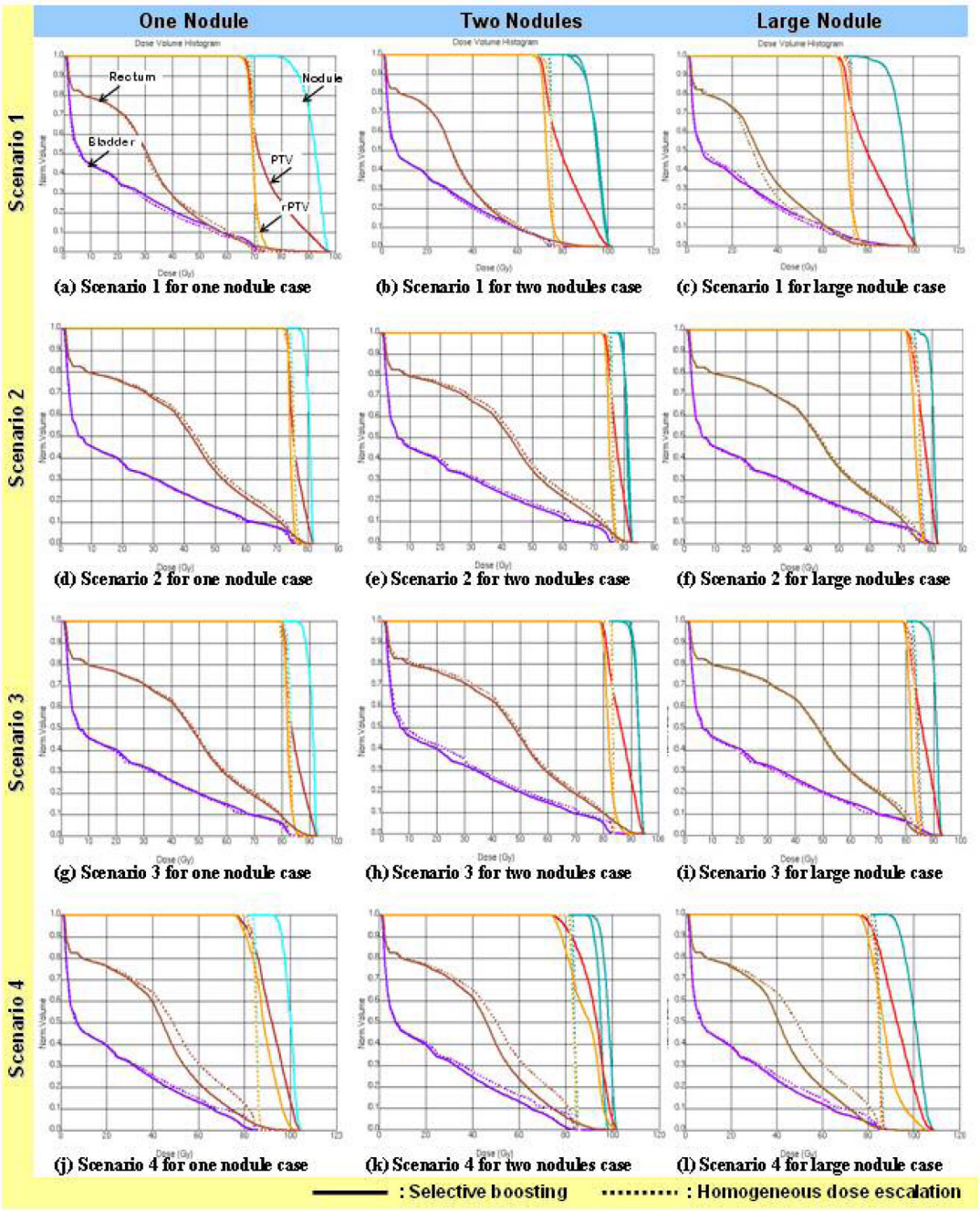

Figure 3.

DVH comparisons for selective boosting IMRT and homogeneous dose escalation IMRT for the four different scenarios and three different high-risk tumor subvolume geometries. As can be seen only risk-adaptive optimization (scenario 4), utilizing radiobiological objective functions shows improved rectal and bladder sparing than it's corresponding homogeneous dose escalation IMRT plan.

Table 1

Four different boosting scenarios employed in the comparison of selective boosting IMRT and homogeneous dose escalation IMRT.

	One nodule [EUD(Gy)]			Two nodules [EUD(Gy)]				Large nodule [EUD(Gy)]			Prescribed Dose
	Nodule	rPTV	PTV	Nodule1	Nodule2	rPTV	PTV	Nodule	rPTV	PTV	
Scenario 1	90	70	71	90	91	72	74	86	70	72	35 fractions of 2 Gy [100% to PTV]
Scenario 2	80	74	75	81	80	75	76	80	74	76	37 fractions of 2 Gy [100% to PTV]
Scenario 3	91	81	82	92	92	81	83	90	81	83	39 fractions of 2 Gy [98% to PTV]
Scenario 4*	98	83	84	97	94	80	83	96	82	84	39 fractions of 2 Gy [100% to PTV]

Abbreviations: EUD = equivalent uniform dose; nodule = a high-risk tumor subvolume; rPTV = a remaining low risk PTV outside nodule;

* risk-adaptive optimization using biological objective functions while selective boosting plans in scenario 1, scenario 2, and scenario 3 employ conventional physical (dose-volume) objective functions.

Acta Oncol. Author manuscript; available in PMC 2009 December 16.

Table 2

NTCP and TCP model parameters used for computations and as risk-adaptive optimization input parameters.

Structures	D_{50} [Gy]	m & n or γ_{50}	References
Organs-at-risk (OAR)			
Bladder	80.0	m = 0.11 & n = 0.5	Burman *et al.*[21]
Unspecific Pelvic Normal tissue	55.0	m = 0.13 & n = 0.15	Burman *et al.*[21]
Rectum (1)	81.9	m = 0.19 & n = 0.23	Rancati *et al.* [20]
Rectum (2)*	75.7	m = 0.14 & n = 0.24	Rancati *et al.* [20]
Rectum (3)*	81.9	m = 0.19 & n = 1.03	Tucker *et al.* [25]
Tumor classification			
Intermediate risk (*M*)	72.8	γ_{50} = 8	
High risk (*H*)	77.3	γ_{50} = 8	Levegrün *et al.* [19]
Very high risk (H_+)	82.3	γ_{50} = 8	

Abbreviations: D_{50} = dose yielding 50 % dose-response for a specific end point to either normal tissue complications or tumor control; γ_{50} = a normalized dose-response gradient; m = the parameter is related to the slope of a dose-response curve $\left(m = 1.6 / 4\gamma_{50}\right)$; n = a volume effect parameter;

*They were added to minimize NTCP model parameter dependency when calculating NTCP values (not used in risk-adaptive optimization process).

Table 3

Shows rectal and bladder sparing for selective boosting and homogeneous dose escalation strategies.

Specificity Level	Bladder (NTCP < 10^{-4}%)			Rectum / Rectal Wall								
	gEUD	% VOL [cc]		gEUD	Rectum (1)	NTCP Rectum (2)	Rectum (3)	% VOL [cc] Receiving				
	[Gy]	65Gy	75GY	[Gy]	[%]	[%]	[%]	40 Gy	50 Gy	60 Gy	70 Gy	75 Gy
One Nodule												
Scenario 1 (Δ)	*−1.4*	*−0.4*	*0.0*	*0.0/−1.3*	*0.0/−0.1*	*0.0/0.0*	*0.0/0.0*	*+2.6/+0.2*	*+4.1/+1.4*	*+2.3/+1.3*	*−2.8/−2.6*	*−1.8/−1.9*
Scenario 2 (Δ)	*−1.1*	*−0.2*	*+1.1*	*+1.3/ +0.8*	*+0.6/+0.2*	*+0.5/+0.1*	*+0.7/+0.1*	*+2.4/+1.9*	*+4.1/+1.3*	*+3.4/+1.1*	*+3.0/+0.9*	*−1.0/−0.6*
Scenario 3 (Δ)	*−0.7*	*−1.4*	*−0.2*	*0.0/+0.3*	*−0.7/+0.1*	*−0.7/+0.1*	*−1.2/0.0*	*−0.5/+1.1*	*−1.9/+1.0*	*0.0/+1.1*	*+0.6/+0.9*	*+0.6/+0.7*
Scenario 4* (Δ)	*+2.0*	*+0.6*	*+2.7*	*+4.9/+2.7*	*+3.7/+0.8*	*+4.2/+0.4*	*+5.3/0.0*	*+4.6/+6.4*	*+11.2/+3.5*	*+9.0/+2.8*	*+8.3/+2.4*	*+8.0/+2.5*
Two Nodules												
Scenario 1 (Δ)	*−0.5*	*−0.7*	*+1.0*	*−1.14/−0.9*	*−0.2/−0.1*	*−0.1/−0.0*	*0.0/0.0*	*−0.7/−0.2*	*+1.6/+1.1*	*+1.74/+1.40*	*−0.9/0.0*	*−3.0/−2.0*
Scenario 2 (Δ)	*+1.4*	*+0.9*	*+5.5*	*+1.1/+1.6*	*+0.6/+0.3*	*+0.5/+0.1*	*+0.1/0.0*	*+2.8/+4.3*	*+2.9/+2.6*	*+2.67/+1.76*	*+2.8/+1.6*	*+0.4/+0.9*
Scenario 3 (Δ)	*+1.6*	*+1.6*	*+0.7*	*−0.1/+0.6*	*−0.1/+0.2*	*−0.1/+0.1*	*+0.1/0.0*	*+2.1/+3.8*	*+1.8/+2.7*	*+1.38/+2.01*	*+1.4/+1.3*	*+1.4/+1.2*
Scenario 4* (Δ)	*+3.2*	*+4.0*	*+4.7*	*+4.0/+2.3*	*+3.4/+0.7*	*+4.0/0.4*	*+0.4/0.0*	*+3.6/+6.3*	*+10.5/+4.9*	*+9.19/+3.46*	*+8.7/+2.5*	*+8.3/+2.8*
Large Nodule												
Scenario 1 (Δ)	*−1.83*	*−2.10*	*−3.27*	*−1.8/−1.3*	*−0.3/−0.1*	*−0.1/0.0*	*0.0/0.0*	*−7.2/−2.8*	*−5.2/−2.2*	*−1.31/−1.04*	*+1.1/+1.1*	*−1.1/−1.0*
Scenario 2 (Δ)	*−1.04*	*−0.47*	*−3.48*	*+0.9/+0.8*	*+0.5/+0.1*	*+0.4/0.0*	*0.0/0.0*	*+0.8/+1.3*	*+1.1/+0.4*	*+1.04/+0.43*	*+2.2/+1.0*	*+2.9/+2.0*
Scenario 3 (Δ)	*−1.21*	*−2.08*	*−0.33*	*+0.9/+0.5*	*+0.8/+0.2*	*+0.9/+0.1*	*0.0/0.0*	*−0.1/−0.1*	*+1.0/+0.1*	*+0.58/+0.01*	*+1.0/+0.3*	*+1.7/+0.4*
Scenario 4* (Δ)	*+2.06*	*+2.23*	*+2.85*	*+6.8/+3.7*	*+4.8/+1.0*	*+5.1/+0.5*	*+0.5/0.0*	*+11.8/+10.7*	*+16.4/+4.2*	*+11.01/+3.04*	*+9.6/+2.5*	*+9.7/+2.7*

Abbreviations: Rectum (1), Rectum (2), Rectum (3) = represent three different NTCP model parameters described in Table 2;

* risk-adaptive optimization using biological objective functions while selective boosting plans in scenario 1, scenario 2, and scenario 3 employ physical (dose-volume) objective functions;

Δ = the difference between homogeneous dose escalation IMRT and selective boosting IMRT (i.e. '+' stands for an increase in homogeneous dose escalation IMRT). In the notation xx.x/yy.y the first number refers to rectal volume and the second to the rectal wall volume.